Customization and Topology Optimization of Compression Casts/Braces on Two-Manifold Surfaces

Yunbo Zhang[a], Tsz-Ho Kwok[b,*]

[a]*Department of Industrial and Systems Engineering, Rochester Institute of Technology, Rochester, New York 14623, USA*
[b]*Department of Mechanical, Industrial and Aerospace Engineering, Concordia University, Montreal, QC H3G 1M8, Canada*

Abstract

This paper applies the topology optimization (TO) technique to the design of custom compression casts/braces on two-manifold mesh surfaces. Conventional braces or casts, usually made of plaster or fiberglass, have the drawbacks of being heavy and unventilated to wear. To reduce the weight and improve the performance of a custom brace, TO methods are adopted to optimize the geometry of the brace in the three-dimensional (3D) space, but they are computationally expensive. Based on our observation that the brace has a much smaller thickness compared to other dimensions and the applied loads are normal forces, this paper presents a novel TO method based on thin plate elements on the two-dimensional manifold (2-manifold) surfaces instead of 3D solid elements. Our working pipeline starts from a 3D scan of a human body represented by a 2-manifold mesh surface, which is the base design domain for the custom brace. Similar to the concept of isoparametric representation, the 3D design domain is mapped onto a two-dimensional (2D) parametric domain. An Finite Element Analysis (FEA) with bending moments is performed on the parameterized 2D design domain, and the Solid Isotropic Material with Penalization (SIMP) method is applied to optimize the pattern in the parametric domain. After the optimized cast/brace is obtained on the 2-manifold mesh surface, a solid model is generated by our design interface and then sent to a 3D printer for fabrication. Compared with the optimization method with solid elements, our method is more efficient and controllable due to the high efficiency of solving FEA in the 2D domain.

Keywords: Compression garment, Customization, Topology optimization, Computer-aided design

1. Introduction

A Compression cast/brace is a garment that is worn and tightly fitted with the human body. It provides support for people to heal from injury or to protect the body during heavy use. The Compression cast/brace has many benefits such as improving circulation to a given area, protecting skin, moderating temperature, speeding up recovery, improving performance, reducing soreness, and preventing the muscles from tightening up. As it is such a great tool to get in better health, it has been used in many applications. For example, the orthotic brace is used for scoliosis treatment or in rehabilitation to provide compression to the bones and ligaments as well as to immobilize the joint in a neutral position, which "theoretically minimizes stress at the repair site" [1]. An ankle brace is worn around the ankle for immobilization while allowing it to heal from sprains and other injuries [2]. A compression belt is a spinal brace worn around the waist that compresses the abdomen, centers the body mass, and effectively decompresses the spine [3]. Similarly, a belly band is a compression garment which resembles a tube top worn over the abdomen of pregnant women. Although they have so many usages, traditional compression braces are customized in a non-effective way and they do not fit the individual human body completely. The main purposes of orthopedic cast/brace consists of immobilizing injured body, and providing steady compression for treatment, which both require that the cast/brace tightly fits the patent's body. However, the traditional casts/braces can't fit to the patients accurately, as they are made manually by the orthopedists based on their experience. Another drawback of traditional casts/braces is that the materials to make the casts/braces are usually more than needed due to the lack of optimization. As a result, the traditional casts/braces are heavy to wear [4], and not good ventilation[5, 6], and thus bring uncomfortableness to patients during the rehabilitation [4, 5, 7, 6].

With the growth of Additive Manufacturing (AM), it enables the production of custom products without increasing in time, material, or cost. Compression casts/braces can also be completely customized based on the shape of the patient's body as well as the corrective needs, such that they are more effective and more comfortable to wear. However, the customization can only be done empirically with the current Computer-Aided Design (CAD) tools. The design process is complicated and time consuming, not even mentioning the challenges in design optimization. With one requirement is light-weight and the function is to provide compression, the goal of this paper is to apply *Topology Optimization* (TO) in the design of compression casts/braces. TO is a mathematical method that minimizes the weight of a structure and meanwhile maximizes the stiffness. However, applying TO in a three-dimensional (3D) space is computationally expensive, and thus the resolution of result is normally very limited.

*Email: tszho.kwok@concordia.ca

We observe that compression is the forces that are normal to the body surface, and most compression garments are tight-fitting with a small thickness compared to other dimensions. This condition fits very well to the thin plate theories from continuum mechanics, so we borrow and take advantage of its theories to reduce the full 3D solid mechanics problem to a two-dimensional (2D) one with bending moments. Specifically, the 2D quadrilateral finite elements are used in this paper to represent the human body surfaces, which constitute a two-dimensional manifold (2-manifold) design domain with a freeform shape. We reformulate the TO in this 2-manifold domain using the thin plate theory. This is a novel and efficient framework to design compression cast/braces using TO. Our technical contribution is summarized as follows:

1. A workflow for 3D scan to 3D printing is developed for an interactive design of custom compression casts/braces considering the light-weight, fitness, and ventilation.
2. An easy-to-use user interface based on curves is adopted to define the design domain on a 2-manifold surface, which guarantees the fitness of the final product. The interface is also used to define the boundary conditions and loads, and convert the optimized design into a printable solid.
3. The plate theory is applied to map the 3D cast/brace design into a 2-manifold domain, in which a bending-based TO is formulated such that the optimized light-weight structure can be computed efficiently.

Several examples are shown in this paper to demonstrate the proposed design framework for compression casts/braces.

The rest of this section briefs the related works. Section 2 gives the problem definition and the overview of the proposed framework. Section 3 presents the interactive design tools on 2-manifold surface, and the details of converting the 3D shapes to 2-manifold domains as well as the TO in 2-manifold domain is discussed in Section 4. Results and examples are shown in Section 5, and the paper is concluded in Section 6.

1.1. Related Works

This paper focuses on the customization and topology optimization of compression braces, and the related works are classified into computational design for custom product, 3D printed orthopedic brace, and structural analysis and optimization.

Computational Design for Custom Product

Recently, custom product design has become a research focus. Customized products outperform over their mass-produced counterparts, as they provide more comfortableness, unique aesthetic appearance, and/or better performance. However, due to the lack of computational tools to support product customization, it requires unnecessary cost and complexity. To improve the efficiency and reduce the cost of customization, computational tools are developed to support custom product design. Wang et al. [8] proposed a volumetric parameterization based method for design automation of custom wearable products. Interactive systems are developed for designing custom wetsuits [9] and regular garments [10], while a curve editing tool [11] enables users to design custom products on 2-manifold mesh surfaces for 3D printing. To ease the effort of the user, the emerging human computer interaction technique – augmented reality – is adopted to design custom glasses [12], footwear [13], and wearable artifacts [14]. We employ the curve-based tool in this paper to the complete the interaction on 2-manifold surface and the specification of the domain.

Non-conventional Orthopedic Cast/Brace

Supported by 3D printing techniques, new 3D printed brace/cast is developed to overcome the limitations of conventional counterparts. These customized 3D printed casts/braces have more fitness, better ventilation and lighter weight [4], and thus bring more comfortableness to the patients who wear them. Cortex [5] is designed as a web-like hollowed cast. A similar design, named Osteoid [7], is combined with low intensity pulsed ultrasound (LIPUS) bone stimulator system. Kim and Jeong [15] proposed a hybrid cast model consisting of an inner structure produced by 3D printing and an outer cover produced by injection molding, while Lin et al. [4] customized a cast with evenly distributed holes and validated their design using FEA. Besides waist cast, Mavroidis et al. [16] developed a pipeline for 3D printing customized ankle-foot orthoses. Although these methods explored the new possibility of custom design brought by 3D printing techniques, they lack the automation in the design process and require heavy manual design operations by experienced CAD users. Moreover, the obtained shapes in existing works cannot be guaranteed to be optimal. The main reasons for these existing method not being optimal are: 1) The existing works require the designers to design the custom cast/brace manually based on their experience, and none of them have the computational design tool as we have, which allows an automatic design with guaranteed fitness; 2) The lightweight structures are again generated based on the designers' experience for the exiting works, while our method determines the material distribution based on the TO results. Therefore, the computational method is in demand to automate the design process of customizing casts and determine the optimal structurally-sound shapes of the casts. Recently, Zhang et al. [6] proposed a computational method for generating custom cast with awareness of thermal-comfortableness. A thermal image is taken and used to guide the distribution and size of centroidal Voronoi cells on the base design domain of the cast. Their work significantly improved the thermal comfortableness of the customized cast. Different from their work, this work is built upon topology optimization method with the focus on reducing the weight and meanwhile maintaining good structurality for compression braces.

Structural Analysis and Optimization

Topology optimization is a mathematical method to optimize material distribution in a given design domain, for the goal of minimizing the weight and maximizing the stiffness of the structure. The common techniques include solid isotropic material with penalization parameterization (SIMP) method [17, 18], level-set method [19], and ground structure method [20]. All these methods highly rely on Finite Element Analysis (FEA). For models with detailed geometric features, FEA requires high computational power and is very time consuming. Research efforts have been made to reduce the computational

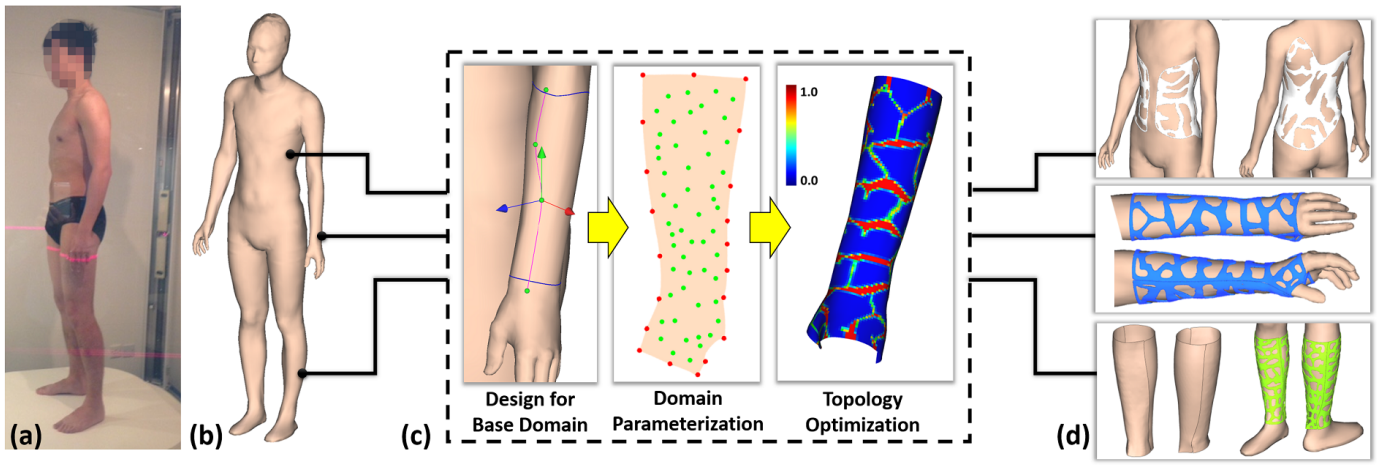

Figure 1. This figure shows a typical workflow for designing a custom compression cast/brace with custom-fit, light-weight and good ventilation, which consists of (a) a laser scanning to acquire the point cloud data of the human body, (b) a surface reconstruction to obtain a 2-manifold mesh surface of the human body, (c) the design domain is interactively defined with the user interface; a base domain parameterization with boundary conditions (indicated as red dots) and distribution loads (indicated as green dots) can also be specified; and the proposed topology optimization is applied on the 2-manifold surface. (d) Three optimized designs: an arm cast, a leg cast and a scoliosis cast.

power consumption and improve the computational efficiency. Some works focus on distributing uni-structures, and optimizing the size and shape of the uni-structures to optimize the structurality of the model [21, 22, 23], while others simplify the formulation of FEA or reformulate it for more efficient solving and lower computation cost [24, 25, 26, 27]. Wu et al. [28] implemented a highly efficient multi-grid FEA solver based upon the Graphics Process Unit (GPU) for high-resolution topology optimization. In this paper, we focus on formulating an efficient TO method on 2-manifold surface for optimizing custom compression cast/brace design. The GPU solver can be integrated in the future to increase the domain resolution and design details.

A recent work [29] proposed a TO framework for 2-manifold surfaces. In their work, they theoretically proved the validity of the idea of solving TO problem on 2-manifold surface. They employed the conformal mapping to map a 2-manifold surface onto a 2D rectangular parametric domain, extended the level-set TO method from 3D Euclidean space to the 2-manifold, and solved the level-set problem in the 2D domain. Actually, our work is motivated by this work, that mathematically proved that a 3D Euclidean TO problem on a 2-manifold surface can be mapped to a 2D parametric domain. While they focused on the development of level-set method, our work aims at the derivation of SIMP method in compression cast/brace design. In addition, ours is an easy-to-use design tool for combining TO and interactive customization on 2-manifold surfaces, which is the first time, to the best of the authors' knowledge.

2. Overview

Currently, most existing Topology Optimization (TO) methods solve the 3D design problem based on 3D solid representations in a 3D Euclidean space $\mathbf{R}^3$ (e.g. volumetric mesh or voxel). However, solving in 3D is computationally expensive, and thus the optimized results have very limited details. In our study, we have two observations: (1) The compression cast/brace are usually made with smaller dimension in thickness than other dimensions, which can be described as a thin plate; (2) The brace generates compression that is normal to the body surface, which can be described as normal loads in the opposite direction. Different from 3D solid representation, 2-manifold defined in the 2D topological space $\mathbf{E}^2$ is another representation of a 3D shape. Actually, the 2-manifold in most cases can be considered as a synonym of a 3D surface [30]. Compared to the computational methods based on 3D solid representation, the ones based on 2-manifold are usually more efficient and require less computational power, due to much less data is required to represent the same shape [31]. With these observations, we hypothesize that if the 3D TO problem for compression cast/brace is solved with a 2-manifold shape representation, the optimization will be more efficient and controllable.

To test our hypothesis, this paper develops a design workflow for customizing compression casts/braces on a 2-manifold human mesh model, from 3D scanning to 3D printing (Fig.1). As TO requires the given design domain, boundary conditions, and applied loads; to apply TO on the 2-manifold domain, there are two challenges: (1) how to interactively specify the design domain on the 2-manifold surface and the loading conditions? (2) how to adapt the existing TO techniques to solve the optimization problem on the 2-manifold surface instead of on 3D solid elements? To address the challenges, briefly, we apply our previous interactive curve-based editing tools [11] to develop an easy-to-use user interface that can support the specification of design domain and loads in arbitrary shapes on the 2-manifold surface; we also apply the thin plate theory of continuum mechanics and the geodesic curve from differential geometry to modify the original TO formulation for the 2-manifold design domain (the geodesic curve is a generalization of a straight line to curved spaces).

The overview of our approach is demonstrated in Fig.1. Firstly, the point cloud data of the body shape is acquired through a 3D scanning (Fig.1(a)). Afterwards, the 3D mesh

model is reconstructed from the point cloud data (Fig.1(b)). Noted that, although a full body scan is used in this paper, it only needs a local scan on the regions of interest if the application does not require a full body scan. Once the 2-manifold surface is obtained, it comes to our major technical contributions as shown in Fig.1(c). The designer can create the design domain by interactively defining curves onto the human model using our user interface. In addition, the boundary conditions and loads can be specified. By applying our TO method onto the 2-manifold surface of the design domain, a customized cast/brace design can be generated with lighter weight, better ventilation, and satisfying designer-specified compression loads. Finally, a ready-to-fabricate solid model can be generated from the 2-manifold domain with our fabrication tool (Fig.1(d)). The technical details of the user interface and the TO formulation are given in the following two sections.

3. User Interface and Fabrication Tools

The prerequisite for applying TO on a 2-manifold surface is the input design domain and boundary conditions defined on the surface, which should be specified by the user. However, different from the Euclidean space $\mathbf{R^3}$ with three orthogonal axes, a 2-manifold $\mathbf{E^2}$ is a topological space defined by the surface of the human body, the interaction of which is not intuitive. A design domain is normally a patch enclosed by its boundaries. Therefore, one way to define the design domain on 2-manifold surface is to specify its boundaries on the surface. As the boundaries can be viewed as a set of curves, we adopt the curve-based interactive tools [11] in this paper to allow users to design custom shapes on a freeform 2-manifold surface via simple interactions. What is needed from the user is just some mouse clicks to define the control points, and the system will automatically complete the curves on the 2-manifold surface. Interested readers can refer to the previous paper [11] for the technical details. This section presents how this tool is applied in the creation of base design domain. The conversion from the zero-volume a 2-manifold design into a printable solid is also presented.

3.1. Design domain on 2-manifold surface

In the Euclidean space, a point is defined by its 3D coordinates (x, y, z), but an alternative representation is required to define a point on a 2-manifold surface. The *attribute node* [32] is applied here, which is associated with not only the 3D position, but also the topology information of the reference model. The attribute node can be classified into *attribute edge node* $\mathbf{p}_{edge}$ and *attribute face node* $\mathbf{p}_{face}$. Each attribute edge node $\mathbf{p}_{edge}$ is defined at the a mesh edge e of the reference model with a parameter $u \in [0, 1]$ associated, and the 3D position of $\mathbf{p}_{edge}$ is computed by interpolating the two endpoints $(\mathbf{p_1}, \mathbf{p_2})$ of e as $\mathbf{p}_{edge} = (1-u)\mathbf{p_1} + u\mathbf{p_2}$. Similarly, the face node $\mathbf{p}_{face}$ is associated with a mesh face with the barycentric coordinates (u, v, w) for a quadrilateral face, where $u, v, w \geq 0$ and $u + v + w \leq 1$. Its 3D position is computed by interpolating the four vertices $(\mathbf{p_1}, \mathbf{p_2}, \mathbf{p_3}, \mathbf{p_4})$ of the quadrilateral face as $\mathbf{p}_{face} = u\mathbf{p_1} + v\mathbf{p_2} + w\mathbf{p_3} + (1-u-v-w)\mathbf{p_4}$. Therefore, a curve defined by attribute edge and face nodes is not only a 3D curve, but also a 2-manifold curve. With this representation, the specification of design domain on 2-manifold surface can be done in four steps as shown in Fig.2.

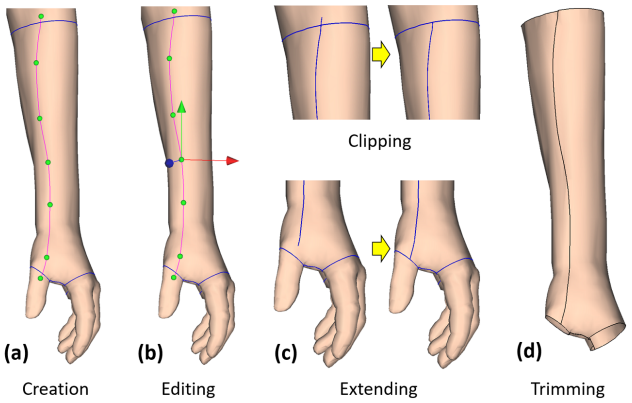

Figure 2. Four steps to specify design domain: (a) A curve is created by picking control points on the reference model. (b) The shape of curve can be edited by changing the positions of control points. (c) The clipping and extending tools make sure each curve touches other curves at its end point. (d) Te design domain can be extracted from the reference model with the curves as the boundaries.

Via simply interactions, a smooth curve tightly fitting to the 2-manifold surface is created by picking control points and conducting the four points interpolation scheme (shown in Fig.2(a)). The created curves can be edited by moving the position of control points on the 2-manifold surface via simply drag-and-drop on a local frame interface (Fig.2(b)). Our design system also provides editing tools such as clipping and extending, to make sure curves touch to each other properly (shown in Fig.2(c)). Once the boundaries are well-defined, the design domain can be extracted from the 2-manifold surface (Fig.2(d)). Here, we apply *Constrained Delaunay Triangulation* (CDT) [33] to triangulate the facets by the points on the curves.

All these operations are simple, easy-to-use, and can be done with an interactive speed [11]. The resultant design domain is well-defined on the 2-manifold surface, so that the fitness of final product is guaranteed.

3.2. From 2-manifold to 3D solid

With the design domain and boundary conditions well-defined on the 2-manifold surface, the design and optimization process can then be conducted, which will be presented in Section 4. However, the result will be defined on this 2-manifold surface, which has zero-volume and is not printable. To introduce a thickness for the result, we applied a thickening operation to convert it into a volumetric model. Briefly, the thickening operation offsets the surface design along the normal direction with a user specified thickness in a *Signed Distance Field* (SDF) [11]. Note that, during the thickening operation, the original surface design is kept as the interface between the volumetric model and the reference human body, and thus the

tight-fitness of the volumetric model to the reference human model is not affected.

Moreover, depending on the mesh resolution of quadrilateral elements, the optimized result may have zigzag regions. Sharp corners and features of compression casts/braces may not be preferred in both structural and aesthetic viewpoints. Therefore, an optional smoothing operation is also supported in our fabrication tool, which should be performed before the thickening operation. The Laplacian operator can be applied to smooth the shapes by moving each vertex to the average position of its neighboring vertices. To make sure the tight-fitness of the final result, the surface-preserved Laplacian smooth is used, i.e., the vertex is moved only if the new position still lies on the original surface.

4. Topology Optimization on Two-Manifold Surface

One of the most commonly used TO technique is the Solid Isotropic Material with Penalization (SIMP) method [18]. Our framework is also built upon SIMP, but it is adapted onto the 2-manifold surface using thin plate theory and geodesic filtering. Before that, the formulation of SIMP is detailed.

4.1. Solid Isotropic Material with Penalization

The SIMP method generates an optimal material distribution in the design domain with respect to the FEA results and total volume constraints. The mathematical formulation of SIMP method can be represented as follows:

$$\begin{aligned} argmin_x \quad & c(x) = \sum_{e=1}^{N} E_e(x_e)\mathbf{u}_e^T\mathbf{k}_0\mathbf{u}_e \\ s.t. \quad & V(x)/V_0 = f \\ & \mathbf{KU} = \mathbf{F} \\ & 0 \le x \le 1, \end{aligned} \tag{1}$$

and

$$E_e(x_e) = E_{min} + x_e^p(E_0 - E_{min}), \tag{2}$$

where $c(x)$ is the total compliance of all elements in the design domain, N is the total number of elements, $\mathbf{u}_e$ is the element displacement vector, $\mathbf{k}_0$ is the is the element stiffness matrix for an element with unit Young's modulus, x_e is the variable to determine the element e's density, E_0 is the Young's modulus of the material, E_{min} is a very small value to prevent stiffness matrix becoming singular, p is a penalty factor, $\mathbf{K}$ is the global stiffness matrix, $\mathbf{U} = \{\mathbf{u}_e\}$ is the global displacement vector, $V(x)$ and V_0 are the optimal volume of material and design domain volume, respectively, and f is the volume fraction set by the user. In order to immobilize the injured body or generate steady compression, the deformation of the cast/brace is undesirable, and therefore, the compliance energy needs to be minimized during the TO computation.

In this formulation, the displacements $\mathbf{u_e}$ and the Young's modulus of elements E_e are dependent on each other, so the minimization is non-linear. This optimization iteratively computes the displacements through $\mathbf{KU} = \mathbf{F}$ using FEA and then updates the Young's modulus distribution. The solution will converge if the compliance $c(x)$ decreases in each step of the iteration. The existing TO methods for 3D solid design domain usually adopt 3D elements for FEA [34], which is computationally expensive. For the design problem of a compression cast/brace, it is possible to map the 2-manifold surface of the brace into a 2D domain, and simplify the general 3D solid FEA problem into a 2D FEA problem. In the next section, the Kirchhoff thin plate theory is applied for FEA using 2D quadrilateral element with normal loads.

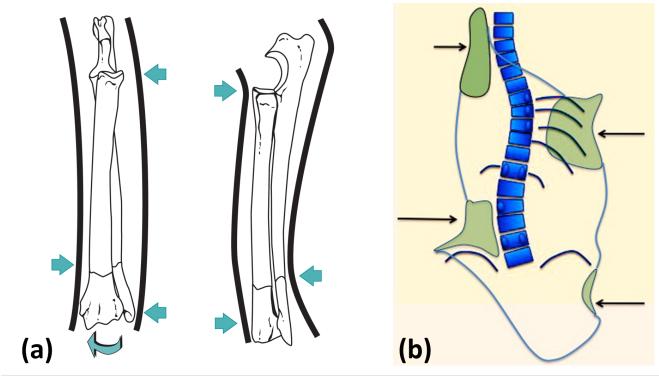

Figure 3. In orthopedic practice, normal load is applied to a arm cast for immobilization (image courtesy of [35]), and a scoliosis brace for the treatment of spine deformation (image courtesy of [36]).

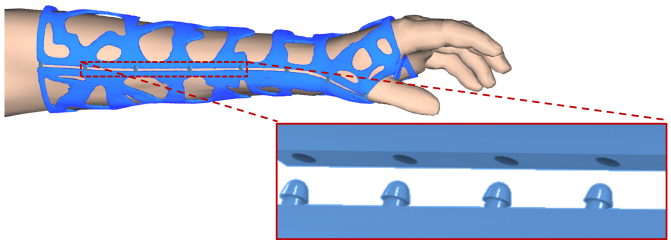

Figure 4. The arm brace design has a front and back pieces, and they are assembled via snap-fits.

4.2. Thin Plate Theory for Two-Manifold Surface

Our target is to design and optimize the compression cast/brace. For the compression cast/brace, we have the following observation: 1) The thickness of the compression cast/brace is far smaller than its other dimensions; 2) As the compression cast/brace is additive-manufactured using PLA materials, which is hardly compressed when wearing the cast/brace, the thickness of the cast/brace is considered to be unchanged; 3) According to the orthopedics practice [35, 36], the compression cast/brace is designed and fabricated to tightly fit to the human body, which generates the steady compression for immobilization of the injured human body or for the treatment of certain orthopedic problems. Therefore the load applied onto the cast/brace in the optimization is normal to the surface of the cast/brace. An efficient way to solve such a FEA problem is the kirchhoff's thin plate theory, which has the following three assumptions:

- The line normal to the neutral axis before bending remains straight after bending. The transverse shearing strains are assumed to be zero, i.e., shear strains γ_{xz} and γ_{yz} are zero.
- The thickness changes can be neglected, and in normal direction, there is no extension. This means normal strain, $\epsilon_z = 0$.
- The normal stress σ_z has no effect on in-plane strains ϵ_x and ϵ_y in the stress-strain equations, and is considered negligible.

The properties of the compression cast/brace satisfy the three assumptions of Kirchhoff's thin plate theory. Moreover, with only normal load applied onto the the compression cast/brace, only in-plane stress and strain exist, which is the same case as that of the 2D plate element. Therefore, we solve the 3D FEA problem using 2D thin plate element.

The boundary conditions of this thin plate based FEA problem also come from the practical requirements of cast/brace.

- **Load** As our work focuses on designing and optimizing compression cast/brace, the load applied to base design domain in the optimization is assumed to be normal to the surface of the design domain but in the opposite direction of the compression.
- **Fixing points** In order to join the two pieces of the cast/brace together, a snap-fit design (see Fig.4)) is adopted. Therefore, the fixing points on the the base design is determined based on the position of the snap-fit.
- **Setting up of the BCs** The normal distribution load is automatically generated by computing a Centroidal Voronoi Diagram (CVD) [37] on the design domain, and then the loads are set onto the site point of each Voronoi region (see green dots in Fig.10). We do allow the user to add extra load after the distribution load applied, by sketching a curve onto the design domain (see the blue dots in Fig.10(b)). This tools improves the flexibility of our system, and enables users' intent of customizing the reinforce regions of the cast/brace design.

The way to specify the loads is important to make loads match the real situation. In the specific examples in our paper, it is assume that the compression forces generated by the cast/brace are evenly distributed. To ensure the evenness, we applied CVD to generate the distributed loads. However, it is not guaranteed that the generated loads best respect the real situation in the current work, as we mainly aim to prove the concept of the presented framework. The study of how the load should be specified would be an interesting future direction to follow up. We plan to set up a physical testing platform to measure the compression forces and their distribution when a person wears a cast/brace.

4.3. Formulation Details of FEA

In this work, we adopt a 4-node quadrilateral element for the discretization of thin plate structures. This element has 4-node and 12 degrees of freedom (shown in Fig. 5). The displacement components of the plate based on Kirchhoff thin plate theory can be expressed with a transverse shear strain [38, 39]

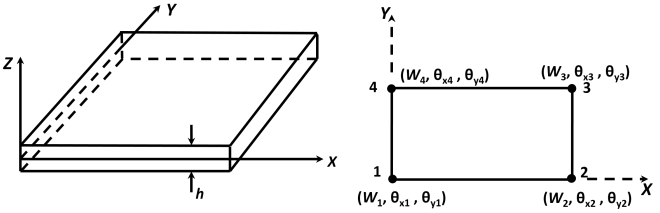

Figure 5. The thin plate element is shown on left-hand side with much smaller dimension of thickness compared to its other dimensions. Based on the Kirchhoff thin plate theory, each element node of an element with only bending has 3-DoFs (w, θ_x, θ_y), where w is w is the transverse displacement, and θ_x and θ_y are the rotations along Y-axes and X-axes respectively.

$$u = -z\frac{\partial w}{\partial x}, \quad v = -z\frac{\partial w}{\partial y}, \quad w = w(x, y), \tag{3}$$

where u and v are the displacement in the x and y axes respectively, w is the transverse displacement, z is the distance from the middle surface ($-h/2 < z < h/2$), and h is the thickness of the plate. With the displacement defined in Eq.3, the stain matrix can be derived as:

$$\epsilon^e = \begin{bmatrix} \epsilon_x \\ \epsilon_y \\ \gamma_{xy} \end{bmatrix} = \begin{bmatrix} -z\frac{\partial^2 w}{\partial x^2} \\ -z\frac{\partial^2 w}{\partial y^2} \\ -z\frac{\partial^2 w}{\partial x \partial y} \end{bmatrix} \tag{4}$$

Based on the Kirchhoff thin plate theory, the two transverse strain γ_{yz} and γ_{zx} can be neglected. The curvature vector κ is related to strain as $\epsilon = z\kappa$. Furthermore, the curvature vector κ is represented as $\kappa = \mathbf{Bu}$, where $\mathbf{B}$ is the strain-displacement matrix and $\mathbf{u}$ is the vector of nodal displacement. Therefore, the stiffness matrix $\mathbf{k}^e$ of each 4-node quadrilateral element can be expressed as follows based on the bending strain energy of the plate:

$$\mathbf{k}^e = \int_A \mathbf{B}^T \mathbf{D} \mathbf{B} dA \tag{5}$$

$$\mathbf{D} = \frac{h^3}{12}\mathbf{C} \tag{6}$$

$$\mathbf{C} = \frac{E}{1-v^2}\begin{bmatrix} 1 & v & 0 \\ v & 0 & 1 \\ 0 & 0 & \frac{1-v}{2} \end{bmatrix} \tag{7}$$

where A, E and v are the area of the element, the Young's modulus, and the Poisson's ratio, respectively. The details for the derivation of the stiffness matrix of the 4-node quadrilateral element are described in Logan's book [40].

To do FEA on the 3D cast/brace model using Kirchhoff thin plate theory, the isoparametric representation [40] is applied to map the 3D element into the 2D parametric domain. For a quadrilateral element of the 3D brace model (highlighted in Fig.6(a)), isoparametric representation maps it from the global

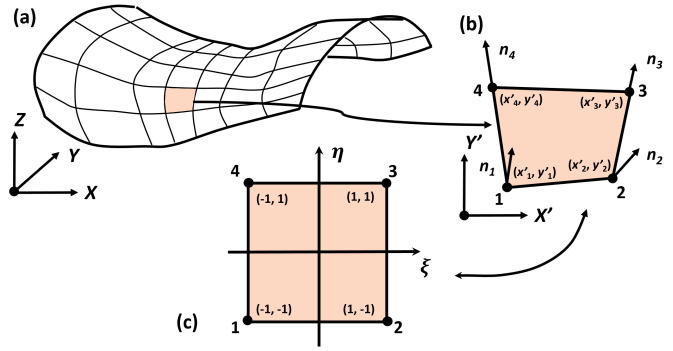

Figure 6. (a) The highlighted element on a 2-manifold surface is transferred to (b) a local coordinate system, and then mapped to (c) the natural coordinate system with two axes ξ and η in the range of [0,1].

3D coordinate system to the so-called natural coordinate system (Fig.6(c)), which is 2D coordinate system with two axes ξ and η ($-1 \leq \xi \leq 1$ and $-1 \leq \eta \leq 1$). In the mapping of the element from global 3D coordinate system to natural coordinate system, there is an intermediate step that firstly maps the 3D element to a local coordinate system defined in the normal plane of the element (Fig.6(b)), and afterwards the mapping between the local coordinate system and the natural coordinate system is established. There exists a point-to-point mapping between the two coordinates, i.e., any point in the natural coordinate system has a corresponding point in 3D global coordinate system on the element, and vice versa. By mapping the 3D quadrilateral elements into 2D natural coordinate system, the Kirchhoff thin plate theory can be applied to solve the FEA on the cast/brace design. This mapping is valid based on the fact that both the element's geometric shape and the displacement use the same shape function (or interpolation function). With the isoparametric representation, the stiffness matrix computed in Eq.5 can be reformulated into

$$\mathbf{k}^e = \int_{-1}^{1}\int_{-1}^{1} (\mathbf{B}_n^T \mathbf{D} \mathbf{B}_n \cdot det(\mathbf{J}) \cdot h) \mathrm{d}\xi \mathrm{d}\eta, \tag{8}$$

where $\mathbf{J}$ is the Jacobian matrix between the local coordinate system and the natural coordinate system, $det(\mathbf{J})$ is the determinant of $\mathbf{J}$, and $\mathbf{B}_n$ shown in Eq.9 is the strain-displacement matrix in terms of ξ and η [40].

$$\begin{bmatrix} \frac{\partial N_1^e}{\partial x} & 0 & 0 & \frac{\partial N_2^e}{\partial x} & 0 & 0 & \frac{\partial N_3^e}{\partial x} & 0 & 0 & \frac{\partial N_4^e}{\partial x} & 0 & 0 \\ 0 & \frac{\partial N_1^e}{\partial y} & 0 & 0 & \frac{\partial N_2^e}{\partial y} & 0 & 0 & \frac{\partial N_3^e}{\partial y} & 0 & 0 & \frac{\partial N_4^e}{\partial y} & 0 \\ \frac{\partial N_1^e}{\partial y} & \frac{\partial N_1^e}{\partial x} & 0 & \frac{\partial N_2^e}{\partial y} & \frac{\partial N_2^e}{\partial x} & 0 & \frac{\partial N_3^e}{\partial y} & \frac{\partial N_3^e}{\partial x} & 0 & \frac{\partial N_4^e}{\partial y} & \frac{\partial N_4^e}{\partial x} & 0 \end{bmatrix} \tag{9}$$

Each partial derivative of $N_j^e, j \in [1,4]$ wrt. x and y can be calculated as:

$$\begin{bmatrix} \frac{\partial N_j}{\partial x} \\ \frac{\partial N_j}{\partial y} \end{bmatrix} = \begin{bmatrix} \frac{\partial x}{\partial \xi} & \frac{\partial y}{\partial \xi} \\ \frac{\partial x}{\partial \eta} & \frac{\partial y}{\partial \eta} \end{bmatrix}^{-1} \begin{bmatrix} \frac{\partial N_j}{\partial \xi} \\ \frac{\partial N_j}{\partial \eta} \end{bmatrix} = \mathbf{J}^{-1} \begin{bmatrix} \frac{\partial N_j}{\partial \xi} \\ \frac{\partial N_j}{\partial \eta} \end{bmatrix}$$

The four shape functions used in Eg.9 are given as follows:

$$N_1^e(\xi,\eta) = \frac{1}{4}(1-\xi)(1-\eta), \quad N_2^e(\xi,\eta) = \frac{1}{4}(1+\xi)(1-\eta),$$

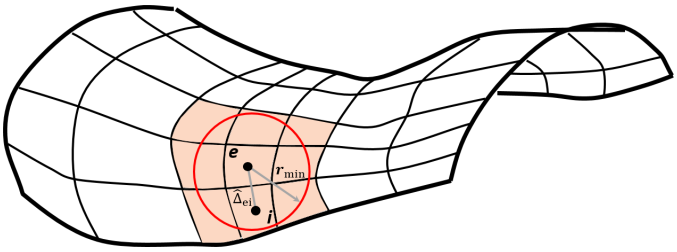

Figure 7. The geodesic filtering computes the weight factor $\widehat{H_{ei}}$ for element i neighboring to element e. Element i is defined as a neighbor of element e if the geodesic distance of between i's centroid and e's centroids is within the user design radius r_{min}.

$$N_3^e(\xi,\eta) = \frac{1}{4}(1+\xi)(1+\eta), \quad N_4^e(\xi,\eta) = \frac{1}{4}(1-\xi)(1+\eta).$$

We integrated the thin-plate FEA solver into the SIMP optimization framework, and therefore $\mathbf{K}$ in Eq.1 is obtained by assembling the element stiffness matrices computed in Eq.8, and $\mathbf{F}$ is the vector of the loads normal to design domain.

4.4. SIMP with Geodesic Filtering

The optimization problem in Eq.1 is solved by a heuristic updating scheme of density variable x_e [18]. This updating scheme relies on the computation of sensitives of cost function $c(x)$ with respect to density variable x_e, which can be represented as

$$\frac{\partial c}{\partial x_e} = -p x_e^{p-1}(E_0 - E_{min}) \mathbf{u}_e^T \mathbf{k}_0 \mathbf{u}_e. \tag{10}$$

To ensure the existence of solutions to the TO problem and to avoid the formation of checkerboard, filters are applied to modify either the sensitive $\frac{\partial c}{\partial x_e}$ or the density x_e. The filtered sensitivity and density are defined as follows [18]:

$$\frac{\widehat{\partial c}}{\partial x_e} = \frac{1}{\max(\gamma, x_e) \sum_{i \in NBR_e} H_{ei}} \sum_{i \in NBR_e} H_{ei} \frac{\partial c}{\partial x_i}, \tag{11}$$

and

$$\widetilde{x_e} = \frac{1}{\sum_{i \in NBR_e} H_{ei}} \sum_{i \in NBR_e} H_{ei} x_i, \tag{12}$$

where NBR_e is the set of neighboring elements to element e, γ is a small positive number to avoid the division by 0, and H_{ei} is the weight factor defined as:

$$H_{ei} = max(0, r_{min} - \Delta(e,i)). \tag{13}$$

r_{min} is the user-specified radius to determine element e's neighbors, and $\Delta(e,i)$ measures the center-to-center distance between element e and each of its neighboring element i. The original SIMP method is developed based on a rectangular design domain, and the design domain is discretized to uniform square quadrilateral element, so the search of neighboring element and computation of the H_{ei} are trivial. However, the weight factor $\widehat{H_{ei}}$ on 2-manifold surface can not be determined by the center-to-center Euclidean distance. To apply SIMP correctly on the 2-manifold mesh surface, this computation of filtering needs to be reformed.

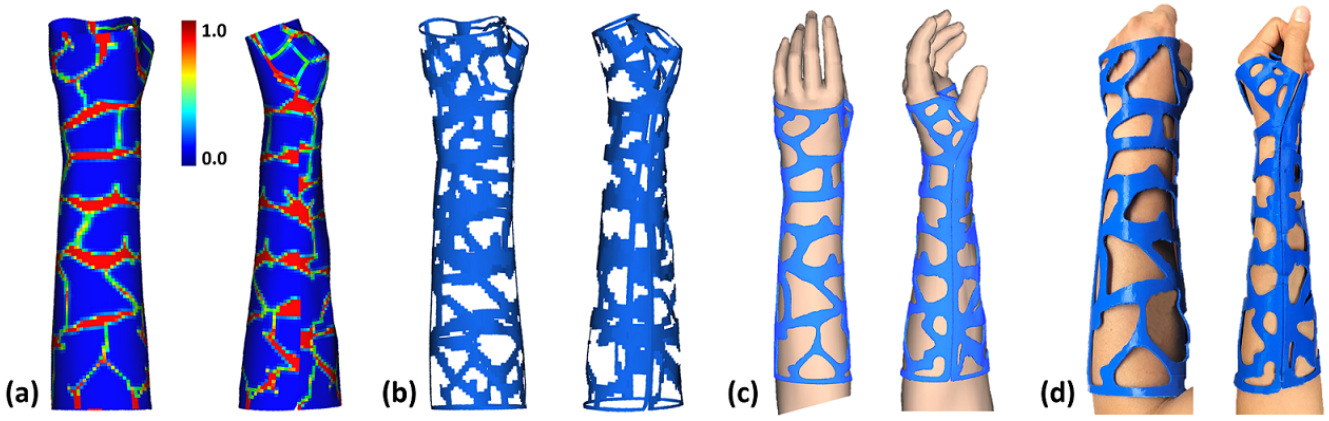

Figure 8. (a) The material density map on the two-manifold brace surface, where the red color means density variable x_e to be 1, and blue means x_e to be 0. (b) Then, the optimized surface design is extracted, (c) smoothed and converted to a volumetric design. (d) The optimized design is prototyped using an Ultimaker2 Fused Deposition Modeling (FDM) printer, and the customized brace is worn by the user with a good fit.

In this paper, we apply the geodesic distance $\widehat{\Delta(e,i)}$ between the center of element e and element i (Fig.7) – named geodesic filtering. To determine $\widehat{\Delta(e,i)}$, we compute a Discrete Exponential Map (DEM) [41] centered at the element e. Based on a Dijkstra's algorithm [42], DEM efficiently computes the geodesic distance between the center element e and its neighboring elements until the distance exceeds r_{min}. The original H_{ei} defined in Eq.13 is then replaced by

$$\widehat{H_{ei}} = max(0, r_{min} - \widehat{\Delta(e,i)}), \tag{14}$$

such that the filtering of sensitivity and density of SIMP method on 2-manifold mesh surface can be realized.

5. Results

We implemented the proposed method using Visual C++ and OpenGL. The linear equation systems in FEA are solved by SuperLU package [43]. All the testing is conducted on a laptop with Inter (R) Core (TM) i7-6600U 2.6-2.8GHz CPU and a 16G RAM, running a 64-bit Windows 10 Enterprise operating system. In all tested examples, we set up the thickness to be $2mm$. To test the proposed geodesic filtering algorithm for SIMP on 2-manifold surface, we set the radius r_{min} of neighboring search on the 2-manifold surface to be 1.2 times the average edge length of the all the elements. For all the physical examples, they are fabricated by an Ultimaker2 FDM printer using Polylactic acid (PLA) as building materials with the Young's modulus of $3500MPa$ and the Poisson ratio of 0.36 [44].

5.1. Customization and tight-fitting

For a compression cast/brace to be effective, it is important being customized to fit the human body. Thanks to the direct design interface on the 2-manifold surface, the resultant product is guaranteed to exactly fit to the human body. The example we tested here is a custom arm cast design. An orthotic arm brace provides compression to the bones and ligaments, and immobilize the joints in a neutral position. The base design domain is obtained using our design tools, and it follows the shape of the human body. Then, the proposed TO method is applied onto the base design domain. To achieve a cast/brace design with light-weight and good ventilation, we set the volume fraction to be 30%, which means only 30% of the material is kept for the optimized design. Following the setting used in Osteoid cast [7], we set up $10N$ distributed load onto the base design domain, and set up the fixed boundary conditions on the boundary to reflect the snap-fit design (see Fig.1(c)). The SIMP result is shown in Fig.8(a) as a density map (red means the density is 1 and blue means 0), which verifies the correctness of the proposed algorithm. As the density value of each element is not a 0-1 binary value, we set a cutoff value 0.01 to remove those elements with a density value less than 0.01. For the converge of the optimization, we adopt the same criteria as [18], and that is: If the change of $\bar{x_e}$ between two steps is smaller than 0.01, the optimization is considered to be converged, where $\bar{x_e}$ is the mean of all element density. This criteria works well for all the examples shown in the paper, and the optimization usually converges within 500 steps except the scoliosis brace (converged at step 764). The customized brace is prototyped using 3D printer and worn on the user's hand as shown in Fig.8(d), which is a perfect fit and validate our framework can customize tight-fitting casts/braces.

5.2. Controllability

We tested the controllability of the proposed method on a leg brace design and a scoliosis design. Although, in general, the applied load is uniformly distributed onto the base design domain, it is possible to have extra load applied onto certain regions for more reinforced structures. For example, we specified some extra loads along a line onto the leg brace to protect the tibia of the leg. As shown in Fig.9(b), besides the distributed load (indicated by green dots), a curve is specified to define extra load (indicated in blue). In our test, we set the distributed load to be $10N$, and the extra load to be $30N$. Compared to the result generated with only distributed load (Fig.9(a)), our

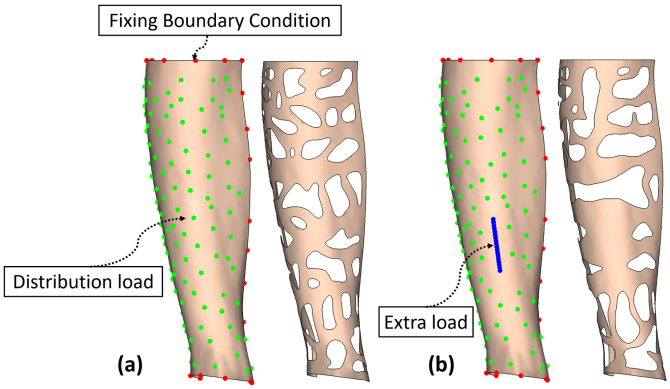

Figure 9. (a) The $10N$ loads are distributed as sampled points on the surfaces of leg cast (indicated by green dots), and the fixed boundary conditions are set on the boundaries of the surfaces (indicated by red dots). (b) A blue curve with $30N$ extra loads is specified by user, and the optimized result well reflects the effect of the extra load.

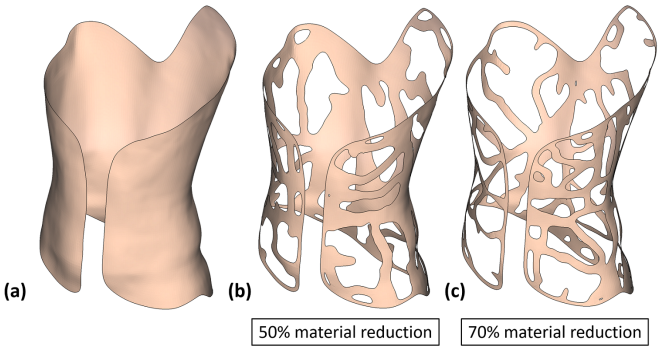

Figure 10. (a) For the design of a scoliosis cast, the volume fraction is set to be (b) 0.5 and (c) 0.3 respectively.

method effectively grows more materials in the region with extra load to reinforce the whole structure, which again affirms the validity and effectiveness of our method for compression cast/brace designs.

We also tested the control of ventilation and material consumption on a scoliosis brace design, through the volume fraction f. The scoliosis brace is used to straighten the spine or trunk deformation on a patient during the phases of rapid growth [45]. The conventional scoliosis brace covers a large area of the patient's upper body, which is heavy and unventilated to wear. Therefore, it is desired to minimize the material consumption of the scoliosis brace to reduce the weight and improve the ventilation. For the scoliosis brace example shown in Fig.10, we set f to be 0.5 (Fig.10 (b)) and 0.3 (Fig.10 (c)).

Both test results verify that our method can effectively adjust the material distribution and ventilation through our easy-to-use user interface. It supports our hypothesis that it is easier to interact and control the optimized shape in the 2-manifold domain.

For the leg cast model with extra load (Fig.9(b)), it takes longer time to converge (2.17 mins) than the one without extra load (1.33 mins). For the scoliosis cast model with 19272 quad elements, it takes 30 mins with the volume fraction of 0.5 and 42 mins with the volume fraction of 0.3.

Table 1. Time statistic of tested models

Model	# Element	Time (mins)
Arm Cast (Front)	4804	1.15
Arm Cast (Back)	4910	1.23
Leg Cast (Front)	4949	1.33 | 2.17[a]
Leg Cast (Back)	4446	1.06
Scoliosis Cast	19272	30 | 42[b]

[a] Time for the one with extra line load.
[b] Time for the one with 0.3 volume fraction.

5.3. Validation&Comparison

To benchmark our method's performance, we conducted a 3D element based TO onto the arm cast model using the Dassault TOSCA system [46]. It takes 2.5 hours to complete the whole computation on the two pieces with 5432 and 5571 hexahedron elements (Fig.11(b)). In Table 1, the time statistic of all the tested models using our method is listed. For the arm and leg cast examples with around 5000 quad elements, it only takes 1 to 2 minutes to process each piece. As TOSCA takes hexahedron elements as input and our method takes quadrilateral elements, the computation comparison may not be an apple-to-apple comparison. We managed to control the number the hexahedron elements to be similar to the number of 2D quadrilateral elements, so that this comparison can reflect the benefit of adopting 2D elements over 3D elements. Compared to the 3D element based TO method, our method has a speedup of around 60 times in computational time. It supports our hypothesis that optimization on 2-manifold surface is more efficient than the one in 3D domain. In order to validate our method, we

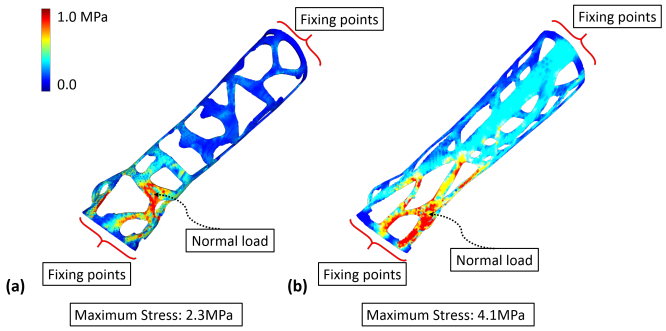

Figure 11. With a normal load and both of the two sides fixed, the FEA [28] is applied onto the result generated by our method (a) and the one by TOSCA (b). A maximum von mises stress 2.3MPa is obtained on (a), while 4.1MPa on (b).

conducted the FEA analysis on both the results generated by our method and the one generated by Dassault TOSCA system. Following [6], we use the 3-point bending test , which requires a normal load applied, and two sides of the model fixed (see Fig.11). To get the high resolution results, we employ the voxel based FEA system [28], with a 256×256 resolution and 1mm

voxel size for the voxelization. As shown in Fig.11, a 30N normal load is applied onto the cast, and both of the two sides of the models are fixed. The color code indicates the von mises stress at each vertex of the voxel, while blue means 0MPa and red means 1.0MPa. Both the color map and maximum stress values suggest our method is superior to the one of TOSCA (2.3MPa vs. 4.1MPa).

6. Conclusion

We proposed a TO method for design and optimization of customized compression casts/braces represented by 2-manifold mesh surfaces. Different from the existing 3D solid element based TO approaches, we observe the thickness of the cast/brace product is much smaller than its other dimensions, and the loads for a compression cast/brace is applied normal to the points on the surface. Based on these two observations, we formulate a 2D thin plate bending FEA to describe the behavior of the compression casts/braces. Compared to the general 3D solid element based FEA, our bending FEA is more computationally efficient. We also adapted the SIMP method, originally based on the regular and planar design domain, to solve the TO problem on 2-manifold surface by proposing a geodesic filtering for the sensitivity and density of SIMP. We tested our method with an arm cast, a leg cast, and a scoliosis brace. The results show our method can successfully and efficiently customize tight-fitting design, reduce the material consumption, and improve ventilation.

In the future, we plan to test our system with more design applications including both compression braces and casts, and adopting GPU based solver [28] to work on designs with even higher resolution. Currently, we don't consider about the window edema caused by wearing a cast/brace for long time. In deed, both the traditional cast/brace and the 3D printed ones usually cause window edema due to the generated compression. A possible way to solve this problem is to add an interior layer made of elastic fabric into the cast/brace. Another future direction could be to incorporate the thermal transmission in the optimization for the better ventilation of the cast/brace. Our method is not applicable to the cast/brace for immobilize or treating joints or other body parts with large relative motion. Therefore, other deformations such as out of plane bending, the membrane, and shear deformations are not considered, but will be in the future. A possible direction to solve these problems is to develop similar objective functions as [29] did for other boundary conditions. A physical platform is also planned to develop for studying the specification of load and verifying the fabricated results.

Acknowledgement

We acknowledge the support of the Natural Sciences & Engineering Research Council of Canada (NSERC) grant # RGPIN-2017-06707. We would also thank Jun Wu from TU Delft for sharing the executable voxel based FEA program.

References

[1] D. J. Slutsky, Techniques in Wrist and Hand Arthroscopy, Elsevier Health Sciences, 2016.
[2] M. Radomski, C. Latham, Occupational Therapy for Physical Dysfunction, Lippincott Williams & Wilkins, 2008.
[3] K.-Y. Chang, S.-C. Chon, The effect of abdominal-compression belt on balance ability with one leg standing, Journal of the Ergonomics Society of Korea 31 (2012) 337–343. doi:10.5143/JESK.2012.31.2.337.
[4] H. Lin, L. Shi, D. Wang, A rapid and intelligent designing technique for patient-specific and 3d-printed orthopedic cast, 3D Printing in Medicine 2 (1) (2015) 4.
[5] Cortex: Exoskeletal cast, `http://www.evilldesign.com/cortex`.
[6] X. Zhang, G. Fang, C. Dai, J. Verlinden, J. Wu, E. Whiting, C. C. L. Wang, Thermal-comfort design of personalized casts, in: Proceedings of the 30th Annual ACM Symposium on User Interface Software and Technology, UIST '17, 2017, pp. 243–254. doi:10.1145/3126594.3126600.
[7] Osteoid medical cast, `https://competition.adesignaward.com/design.php?ID=34151`.
[8] C. C. L. Wang, K.-C. Hui, K.-M. Tong, Volume parameterization for design automation of customized free-form products, IEEE transactions on automation science and engineering 4 (1) (2007) 11–21.
[9] C. C. L. Wang, From designing products to fabricating them from planar materials, IEEE computer graphics and applications 30 (6) (2010) 74–85.
[10] S. Lu, P. Mok, X. Jin, A new design concept: 3d to 2d textile pattern design for garments, Computer-Aided Design 89 (2017) 35–49.
[11] Y. Zhang, T. H. Kwok, An interactive product customization framework for freeform shapes, Rapid Prototyping Journal 23 (6) (2017) 1136–1145.
[12] S.-H. Huang, Y.-I. Yang, C.-H. Chu, Human-centric design personalization of 3d glasses frame in markerless augmented reality, Advanced Engineering Informatics 26 (1) (2012) 35–45.
[13] Y.-I. Yang, C.-K. Yang, C.-H. Chu, A virtual try-on system in augmented reality using rgb-d cameras for footwear personalization, Journal of Manufacturing Systems 33 (4) (2014) 690–698.
[14] M. Gannon, T. Grossman, G. Fitzmaurice, Exoskin: On-body fabrication, in: Proceedings of the 2016 CHI Conference on Human Factors in Computing Systems, ACM, 2016, pp. 5996–6007.
[15] H. Kim, S. Jeong, Case study: Hybrid model for the customized wrist orthosis using 3d printing, Journal of mechanical science and technology 29 (12) (2015) 5151–5156.
[16] C. Mavroidis, R. G. Ranky, M. L. Sivak, B. L. Patritti, J. DiPisa, A. Caddle, K. Gilhooly, L. Govoni, S. Sivak, M. Lancia, et al., Patient specific ankle-foot orthoses using rapid prototyping, Journal of neuroengineering and rehabilitation 8 (1) (2011) 1.
[17] O. Sigmund, A 99 line topology optimization code written in matlab, Structural and multidisciplinary optimization 21 (2) (2001) 120–127.
[18] E. Andreassen, A. Clausen, M. Schevenels, B. S. Lazarov, O. Sigmund, Efficient topology optimization in matlab using 88 lines of code, Structural and Multidisciplinary Optimization 43 (1) (2011) 1–16.
[19] M. Y. Wang, X. Wang, D. Guo, A level set method for structural topology optimization, Computer methods in applied mechanics and engineering 192 (1-2) (2003) 227–246.
[20] W. Dorn, E. Gomory, H. Greenberg, Automatic design of optimal structures, Journal de Mecanique 3 (1964) 25–52.
[21] J. Panetta, Q. Zhou, L. Malomo, N. Pietroni, P. Cignoni, D. Zorin, Elastic textures for additive fabrication, ACM Transactions on Graphics (TOG) 34 (4) (2015) 135.
[22] C. Schumacher, B. Bickel, J. Rys, S. Marschner, C. Daraio, M. Gross, Microstructures to control elasticity in 3d printing, ACM Transactions on Graphics (TOG) 34 (4) (2015) 136.
[23] J. Martínez, J. Dumas, S. Lefebvre, Procedural voronoi foams for additive manufacturing, ACM Transactions on Graphics (TOG) 35 (4) (2016) 44.
[24] Q. Zhou, J. Panetta, D. Zorin, Worst-case structural analysis., ACM Trans. Graph. 32 (4) (2013) 137–1.
[25] D. Chen, D. I. Levin, S. Sueda, W. Matusik, Data-driven finite elements for geometry and material design, ACM Transactions on Graphics (TOG) 34 (4) (2015) 74.
[26] P. Musialski, C. Hafner, F. Rist, M. Birsak, M. Wimmer, L. Kobbelt, Nonlinear shape optimization using local subspace projections, ACM Transactions on Graphics (TOG) 35 (4) (2016) 87.
[27] T. Langlois, A. Shamir, D. Dror, W. Matusik, D. I. Levin, Stochastic struc-

tural analysis for context-aware design and fabrication, ACM Transactions on Graphics (TOG) 35 (6) (2016) 226.
[28] J. Wu, C. Dick, R. Westermann, A system for high-resolution topology optimization, IEEE transactions on visualization and computer graphics 22 (3) (2016) 1195–1208.
[29] Q. Ye, Y. Guo, S. Chen, N. Lei, X. D. Gu, Topology optimization of conformal structures on manifolds using extended level set methods (x-lsm) and conformal geometry theory, Computer Methods in Applied Mechanics and Engineering 344 (2019) 164–185.
[30] M. P. Do Carmo, Differential Geometry of Curves and Surfaces: Revised and Updated Second Edition, Courier Dover Publications, 2016.
[31] M. Botsch, L. Kobbelt, M. Pauly, P. Alliez, B. Lévy, Polygon mesh processing, CRC press, 2010.
[32] C. C. L. Wang, Cybertape: an interactive measurement tool on polyhedral surface, Computers & Graphics 28 (5) (2004) 731–745.
[33] J. Mitani, A simple-to-implement method for cutting a mesh model by a hand-drawn stroke, in: Proceedings of the 2nd EUROGRAPHICS Workshop on Sketch-Based Interfaces and Modeling, 2005, pp. 35–41.
[34] K. Liu, A. Tovar, An efficient 3d topology optimization code written in matlab, Structural and Multidisciplinary Optimization 50 (6) (2014) 1175–1196.
[35] M. A. Keller, P. M. Montavon, Conservative fracture treatment using casts: indications, principles of closed fracture reduction and stabilization, and cast materials, COMPENDIUM.
[36] M. Rigo, M. Jelačić, Brace technology thematic series: the 3d rigo chêneau-type brace, Scoliosis and spinal disorders 12 (1) (2017) 10.
[37] Q. Du, V. Faber, M. Gunzburger, Centroidal voronoi tessellations: Applications and algorithms, SIAM review 41 (4) (1999) 637–676.
[38] E. Reissner, On the theory of transverse bending of elastic plates, International Journal of Solids and Structures 12 (8) (1976) 545–554.
[39] R. D. Mindlin, Influence of rotatory inertia and shear on flexural motions of isotropic, elastic plates, J. appl. Mech. 18 (1951) 31.
[40] D. L. Logan, A first course in the finite element method, Cengage Learning, 2011.
[41] R. Schmidt, C. Grimm, B. Wyvill, Interactive decal compositing with discrete exponential maps, in: ACM Transactions on Graphics (TOG), Vol. 25, ACM, 2006, pp. 605–613.
[42] E. W. Dijkstra, A note on two problems in connexion with graphs, Numerische mathematik 1 (1) (1959) 269–271.
[43] X. S. Li, An overview of superlu: Algorithms, implementation, and user interface, ACM Transactions on Mathematical Software (TOMS) 31 (3) (2005) 302–325.
[44] J. Torres, J. Cotelo, J. Karl, A. P. Gordon, Mechanical property optimization of fdm pla in shear with multiple objectives, Jom 67 (5) (2015) 1183–1193.
[45] H. Weiss, S. Seibel, M. Moramarco, A. Kleban, Bracing scoliosis: the evolution to cad/cam for improved in-brace corrections, Hard Tissue 2 (5) (2013) 43.
[46] Tosca, `https://www.3ds.com/products-services/simulia/products/tosca/structure/topology-optimization/`.